EFFECTS OF STRESS-DEPENDENT SOIL-WATER CHARACTERISTIC AND DAMMING ON SLOPE STABILITY

C. W. W. Ng, The Hong Kong University of Science and Technology, Hong Kong
J. C. H. Lai, The Hong Kong University of Science and Technology, Hong Kong

ABSTRACT
Conventionally a drying soil water characteristic curve (SWCC) is adopted in numerical transient seepage analysis of an initially unsaturated soil slope. The drying SWCC used is generally determined under zero net normal stress and the soil slope is assumed to be homogenous without the presence of any hydraulic obstacles such as large-diameter concrete piles. Obviously soil in a slope is subjected to different stress states at different locations in the field. In this paper, three series of numerical simulations are carried out to investigate the effects of wetting path and stress-dependency of SWCC (SDSWCC) on pore water pressure distributions and hence factor of safety of an initially unsaturated soil slope when it is subjected to a prolonged 10-day rainfall. In addition, damming effects on pore water pressure distributions due to the presence of two piles are studied.

RESUME
Effets sur la stabilité de pente d'une courbe caractéristique Sol-Eau dépendant de la contrainte

1. INTRODUCTION

Rainfall induced landslides are one of the most concerned natural disasters in many parts of the world. Many numerical studies have been conducted to investigate effects of rainfall infiltration on transient seepage and slope stability (Anderson and Pope 1984; Lam et al. 1987; Fredlund and Barbour 1992; Rahardjo and Leong 1997; Ng and Shi 1998; Ng et al. 2001). In a numerical transient seepage analysis of a homogenous unsaturated soil slope, two essential hydraulic parameters are required: a soil-water characteristic curve (SWCC) and a mathematical function relating water permeability and soil suction. Conventionally, a drying SWCC of an unsaturated soil specimen is measured under zero net normal stress condition. Volume change of the soil specimen during the drying process is neglected when volumetric water content is calculated. The measured drying SWCC is then adopted for transient seepage analysis. However, soil elements at different depths in an actual slope experience different stress states, and they normally have been subjected to many drying and wetting cycles due to climatic changes throughout the years. It is no doubt that volume changes would have taken place in these soil elements during the drying and wetting cycles. To account for stress effects and volume changes during a wetting and drying cycle, Ng and Pang (2000) conducted an experimental study to investigate the influences of stress state on a SWCC with volume change measurements. Their test results clearly demonstrate that soil-water characteristic of a volcanic fine grain soil is stress-dependent. Thus, stress-dependent soil-water characteristic curve (SDSWCC) should be used in transient seepage analysis of a homogenous unsaturated soil slope. For non-homogenous slopes due to the presence of some artificial hydraulic obstructions such as large diameter piles, it is a general perception that these obstructions will dam the groundwater flow and hence they will adversely affect the stability of the slopes. However, relatively little research has been carried out to investigate the influence of artificial obstruction on transient seepage and hence slope stability in unsaturated soils.

The objectives of this paper are to study any difference in computed pore water pressure distributions using drying SWCC, wetting SWCC and wetting SDSWCC and to investigate damming effects (if any) on pore-water pressure distributions and slope stability due to the presence of piles in an initially unsaturated soil slope.

2. TRANSIENT SEEPAGE ANALYSES

In order to investigate the importance of SDSWCC and damming effects on the predictions of pore water pressure distributions, three series of parametric numerical analyses are carried out using the finite element program SEEP/W (Geo-slope, 2002). An unsaturated natural slope in Hong Kong is selected for these parametric analyses.

2.1 Seepage in unsaturated soils

Flow of water through a saturated or unsaturated soil is governed by Darcy's law. For an unsaturated soil, the coefficient of water permeability cannot be assumed to be

a constant any longer. As the water content of a soil decreases, the coefficient of water permeability also decreases. The governing partial differential equation for water flow through a two-dimensional unsaturated soil element is given by Lam et al. (1987) as follows:

$$\frac{\partial}{\partial x}\left(k_x \frac{\partial h}{\partial x}\right)+\frac{\partial}{\partial y}\left(k_y \frac{\partial h}{\partial y}\right)=m_w\left(\frac{\partial u_w}{\partial t}\right) \quad [1]$$

where
h = total hydraulic head
k_x = water permeability in the x-direction
k_y = water permeability in the y-direction
m_w = slope of a SWCC
u_w = pore-water pressure

A SWCC and a water permeability function are essential input functions for a transient seepage analysis. In this study, soil is assumed to be homogenous and isotropic (i.e. k_x is equal to k_y).

2.2 Soil water characteristic curves

The measured soil water characteristics of a natural (or so-called undisturbed) volcanic soil reported by Ng and Pang (2000) are adopted in this paper. For investigating the influence of one-dimensional (K_o) stress state on SWCC, Ng and Pang (2000) developed a stress controllable pressure plate extractor. The net normal stress can be controlled one-dimensionally and axial deformation can be measured using the extractor. The soil used by them was a completely decomposed volcanic (CDV) soil, which was taken in form of three soil blocks excavated from a slope in Shatin, Hong Kong. According to GEOGUIDE (1988), the soil can be described as a firm, moist, orangish brown, slightly sandy silt/clay with high plasticity. The gravel, sand, silt and clay contents are 4.9, 20.1, 36.6, and 37.1%, respectively.

The net normal stresses considered in the paper are 0, 40 and 80 kPa, which are appropriate for many relatively shallow slope failures in Hong Kong. Three natural or undisturbed specimens (70 mm in diameter and 20 mm in height) were directly cut from the block samples into three oedometer rings (Ng and Pang 2000). These specimens were first saturated, and then placed in a volumetric pressure plate extractor to determine SWCC under zero net normal stress (CDV-N1) and in the stress controllable pressure plate extractor for measuring SDSWCCs under vertically applied net normal stresses of 40 kPa (CDV-N2) and 80 kPa (CDV-N3).

Figure 1 shows the measured SWCCs and SDSWCCs. As expected, a CDV specimen loaded to a higher net normal stress exhibits a lower initial volumetric water content at suction equal to 0.1 kPa. As the matric suction increases, the volumetric water content of all specimens decreases but at different de-saturation rates. The higher the applied load acting on a specimen, the lower the de-saturation rate. There is a general and consistent trend for a soil specimen possessing a larger air-entry value when it is subjected to a higher stress. The air-entry values estimated from CDV-N1, CDV-N2 and CDV-N3 are 1.5, 3 and 5kPa, respectively. There is a marked hysteresis between a drying and wetting curve for all soil specimens tested. However, the size of the hysteresis loops does not seem to be dependent on the net normal stresses considered. By fitting some relevant measured data with Fredlund and Xing (1994)'s equation, four idealized SWCCs and SDSWCCs for numerical analyses are shown in Figure 2. Details of the use of these idealized curves and a numerical parametric analysis plan are discussed later.

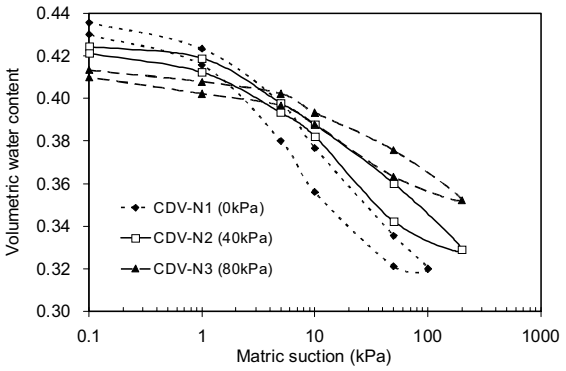

Figure 1. Influence of stress state on soil-water characteristics of natural CDV specimens (from Ng and Pang 2000)

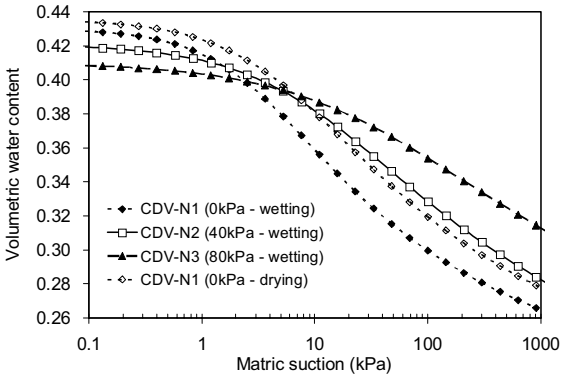

Figure 2. Fitted soil-water characteristic curves from measurements of CDV specimens

2.3 Permeability functions

With the curved fitted SWCC and SDSWCCs shown in Figure 2 and the measured saturated water permeability k_s of the soil in a triaxial apparatus under appropriate stress conditions (Ng and Pang 1998), water permeability functions for different stress states are derived using the procedures proposed by Fredlund et al. (1994) and a computer software called SoilVision (SoilVision, 2002). The empirically derived water permeability functions are shown in Figure 3. As expected, a soil specimen loaded to a higher net normal stress has a lower water permeability

at a given suction. This is because an application of net normal stress has resulted in a smaller pore size distribution inside the soil specimen.

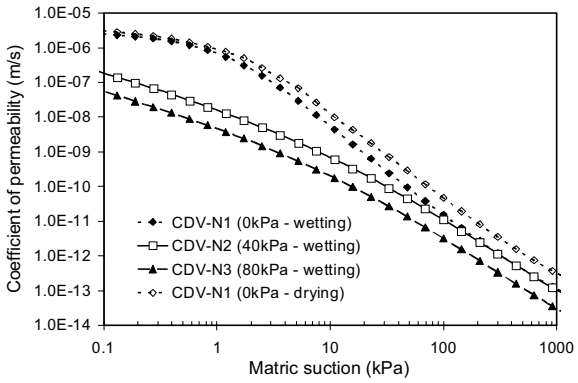

Figure 3. Water permeability functions derived from the measured soil water characteristics of natural CDV soil

2.4 Finite element mesh and numerical analysis plan

An initially unsaturated natural soil slope located in Hong Kong is chosen for this idealized parametric study. The slope inclines at approximately 26° to the horizontal. Figure 4 shows a dimensional finite element mesh of the slope. The 20m thick CDV soil mass is idealized into three different soil layers according to their approximate stress states so that the measured SWCC and SDSWCCs and their corresponding water permeability functions can be specified. To study damming effects due to construction obstructions on pore-water pressure distributions, two artificial hydraulic barriers such as piles are simulated in some cases. The diameter and depth of the two piles is 1m and 6m, respectively. They are 16m apart as shown in Figure 4. It should be noted that the two artificial hydraulic obstructions essentially behave as an infinite long 6m deep impervious retaining wall in the two-dimensional seepage analyses. In other words, damming effects are very likely to be overestimated in this study, unless a three-dimensional transient seepage analysis can be carried out (Ng et al. 2001).

To investigate the influence of wetting SWCC and effects of stress states (i.e., SDSWCCs) on pore-water pressure distributions, three series of transient seepage analyses are conducted. Series D consists of "conventional" transient analyses in which the drying path of the SWCC (CDV-N1) under zero net normal stress and its corresponding water permeability function are specified for all the three soil layers in the slope. In Series W, since rainfall infiltration into the soil slope is a wetting process, all soil layers are assumed to have the same wetting SWCC (CDV-N1) under zero net normal stress and the corresponding permeability

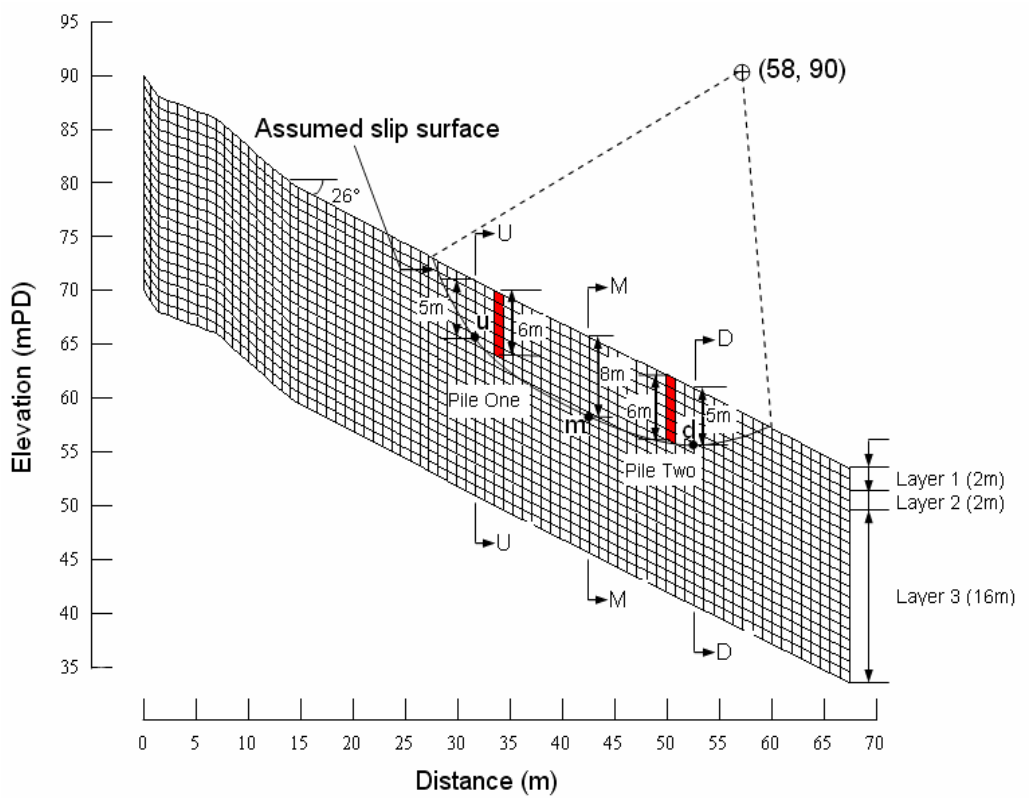

Figure 4. Finite element mesh and slip surface considered in slope stability analysis

function. In Series SW, the measured wetting SWCC (CDV-N1) at zero stress and SDSWCCs (CDV-N2 and N3) are specified for soil layers 1, 2 and 3, respectively, for investigating the influence of stress-dependency of soil-water characteristics on transient seepage analyses. A summary of the three series of analyses is given in Table 1. For each series, there are four cases considered to study damming effect (if any) caused by the two pile obstructions. Case (a) is a reference run, in which no pile is installed in the slope. In Case (b), a pile, i.e., Pile One, is installed at the upstream only (see Figure 4). Similarly, Case (c) is to determine damming effect caused by Pile Two installed at downstream only. Case (d) is for studying damming effect caused by the two piles installed at both upstream and downstream, located at 16m apart.

Table 1. Summary of numerical simulation plan

Series	Analysis Identity	Pile One	Pile Two	Soil-water characteristic
D	D-a	N	N	CDV-N1(drying)
	D-b	Y	N	
	D-c	N	Y	
	D-d	Y	Y	
W	W-a	N	N	CDV-N1(wetting)
	W-b	Y	N	
	W-c	N	Y	
	W-d	Y	Y	
SW	SW-a	N	N	CDV-N1 (wetting)
	SW-b	Y	N	CDV-N2 (wetting at 40kPa)
	SW-c	N	Y	CDV-N3 (wetting at 80kPa)
	SW-d	Y	Y	

Note: Average rainfall intensity of 49 mm/day are applied for 10 days
D = Drying curve at zero stress
W = Wetting curve at zero stress
SW = Stress dependent wetting curves
N = Pile is not constructed, Y = Pile is constructed

2.5 Numerical simulation procedures and hydraulic boundary conditions

Prior to each transient seepage analysis, a steady-state analysis is carried out to establish the initial pore water distributions in the slope. This is done by applying a uniform rainfall intensity of 0.01 mm/day (or 1.16×10^{-10} m/sec) on the top of the slope surface. At the right boundary of the mesh (see Figure 4), a constant hydraulic head of 47.6m above the Principal Datum (or 47.6 mPD above sea level) is specified. This specified head is based on pore water pressure measured by a piezometer at the site of the selected slope. The bottom hydraulic boundary is assumed to be impermeable, and no flux boundary is specified along the left boundary of the mesh. For the cases with piles installed, the piles are modeled as an almost impermeable obstruction with a constant water permeability of 1.0×10^{-15} m/s.

During any transient seepage analysis, an average rainfall intensity of 82mm/day is adopted. The average intensity used is based on actual measurements of rainfall intensity for a 10-year return period spanning from 1980 to 1990 in Hong Kong (Lam and Leung 1995). To allow for surface run off, it is assumed that the average rate of infiltration is equal to 60% of the average rainfall intensity (Tung et al. 1999). In the numerical simulations, infiltration due to rainfall is thus modelled by applying a surface flux of 49mm/day or 5.7×10^{-7} m/sec (i.e. 60% of 82mm/day) across the top boundary surface of the slope for 10 days continuously in each case to simulate a prolonged rainfall event.

3. SLOPE STABILITY ANALYSES

After pore-water pressure distributions within the slope are computed from the transient seepage analyses, factor of safety (FOS) of the slope is determined by carrying out limit equilibrium analysis using a computer software called, SLOPE/W (Geo-slope, 2002). In this software, computed pore water pressures from SEEP/W are used as input parameters for slope stability calculations.

3.1 Shear Strength for saturated/unsaturated soils

To define shear failure of an unsaturated soil, an extension of Mohr-Coulomb failure criterion proposed by Fredlund et al. (1978) is used in this paper as given in the following equation:

$$\tau = c' + (\sigma - u_a) \tan \phi' + (u_a - u_w) \tan \phi^b \quad [2]$$

where
τ = shear stress on the failure plane at failure
c' = effective cohesion
ϕ' = effective angle of internal friction
ϕ^b = angle indicating the rate of increase in shear strength with respect to matric suction.

The failure criterion is governed by two independent stress state variables of net normal stress, $\sigma - u_a$, and matric suction, $u_a - u_w$. It has three parameters, c', ϕ' and ϕ^b.

3.2 Input parameters and procedures for slope stability analyses

For calculating factor of safety (FOS) for each case, the Janbu's simplified method is used together with the extended Mohr Coulomb failure criterion. The shear-strength parameters used include an effective cohesion c' of 2kPa, an effective angle of friction ϕ' of 28°, and an angle (ϕ^b) of 14° which indicates the rate of an increase in shear strength with respect to matric suction. Limit equilibrium analyses are performed on a selected noncircular slip surface (see Figure 4). It should be noted the selected slip surface does not necessarily give the lowest FOS for each case. The selection of a slip surface is merely to compare relative FOSs computed for difference cases considered as given in Table 1. As shown in Figure 4, locations "u", "m" and "d" represent the intersections of the assumed slip surface and sections U-U, M-M and D-D, respectively.

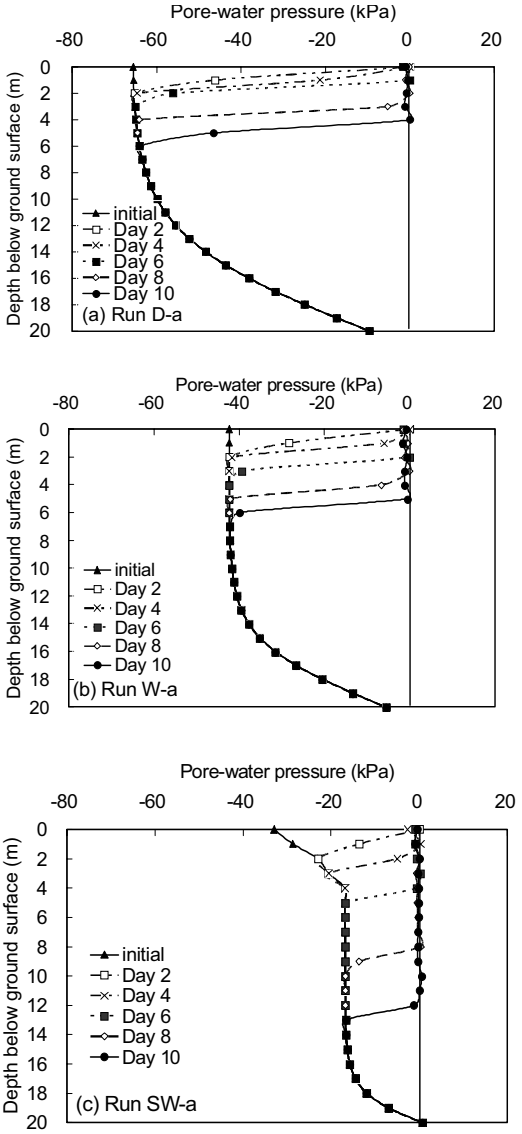

Figure 5. Pore-water pressure distributions along Section U-U

4. INTERPRETATIONS OF COMPUTED RESULTS

4.1 Influences of wetting SWCC and SDSWCC on pore-water pressure distributions

Figures 5a to 5c show the computed distributions of pore-water pressure with depth along section U-U of the slope without any pile obstruction (i.e., Run D-a, Run W-a and Run SW-a as summarized in Table 1). It is clear that there is a substantial difference among the initial pore-water pressure distributions computed using the drying SWCCs (Run D-a), the wetting SWCCs (Run W-a) and the SDSWCCs (Run SW-a) in the three steady-state analyses. Run D-a predicts a much higher soil suction profile than that computed by the other two unconventional analyses (Run W-a and Run SW-a). This is because at the steady state the mobilized water permeability in the soil slope is close or equal to the applied constant infiltration rate of 0.01 mm/day (or 1.16×10^{-10} m/sec) when a hydraulic gradient of unity or close to unity is set-up for a soil zone near the ground surface. In other words, as shown in Figure 3, for the given constant infiltration rate of 1.16×10^{-10} m/sec or mobilized water permeability, the corresponding soil suction calculated in Run D-a using the drying CDV-N1 permeability function is higher than that of Run W-a using the wetting CDV-N1 permeability function, which in terms is higher than that of Run SW-a using the wetting CDV-N1, N2 and N3 permeability functions.

In the transient analyses of the 10-day prolonged rainfall with the constant intensity of 49mm/day (or 5.7×10^{-7} m/sec), a wetting front is formed and it moves progressively downward as the rainfall continues in all three runs as shown in Figure 5. In comparing the computed results of using a drying SWCC (i.e., Run D-a) and a wetting SWCC (i.e., Run W-a) at Day 10, the wetting front of Run W-a penetrates about 1m deeper than that of Run D-a (Figures 5a and 5b). This is because the initial soil suction in Run W-a is lower and hence the soil is more permeable for the advancement of the wetting front. Rahardjo and Leong (1997) conducted two similar analyses to study the difference in transient seepage analyses of rainfall infiltration using a drying and a wetting SWCC. In their two analyses, however, they specified an identical initial pore water pressure distribution. They reported that the analysis using a wetting SWCC produced a shallower wetting front, which is not consistent to the results shown in Figure 5.

When SDSWCCs are considered, the wetting front in Run SW-a penetrates about 13m below ground at Day 10 (see Figure 5c). This is substantially deeper than the computed 5m depth in Run D-a and 6m depth in Run W-a. For the hydraulic parameters and geometry of the slope considered in this paper, SDSWCCs clearly facilitate the advancement of the wetting front into the soil at great depths and lead to significant reduction in soil suction. These could have some devastating adverse effects on slope stability. Therefore, neglecting the influence of stress state on SWCC in a transient seepage analysis could result in non-conservative slope stability calculations.

4.2 Damming effect on pore-water pressure distributions

Since transient seepage analyses using SDSWCCs are theoretically correct and relevant to geotechnical engineering problems, only computed results from series SW are chosen to illustrate any damming effect due to the presence of some hydraulic obstructions on pore water pressure distributions. It should be reminded that a summary of different arrangement of the two hydraulic obstructions (i.e., piles) in series SW is given in Table 1. Figure 6 shows the computed changes of hydraulic head at locations “u”, “m” and “d”. The depths of locations “u”, “m” and “d” are 5m, 8m and 5m, respectively (refer to Figure 4). At location “u”, due to the presence of Pile One in Run SW-b and Run SW-d, the subsurface seepage at

the upstream has been dammed in these two analyses. Therefore, the initial hydraulic heads computed in Run SW-b and Run SW-d are slightly higher than those of SW-a and SW-c (Figure 6a). During the first five days of rainfall (Day 1 to Day 5), there is no significant change in hydraulic head in all four cases considered. This is because there is not enough time for a wetting front to reach location “u”. As shown in Figure 7a, the wetting fronts of all the analyses are still above the level of location “u” on Day 5. It should be noted that the wetting front of Run SW-b penetrates slightly deeper than that of Run SW-a (see Figure 7a) since seepage at the upstream face of Pile One is dammed by the pile in Run SW-b. The dammed water is forced to flow downward around the pile tip. As the computed results of Run SW-c and Run SW-d are similar to those of Run SW-a and Run SW-b respectively, therefore only the results from latter two runs are shown for clarity.

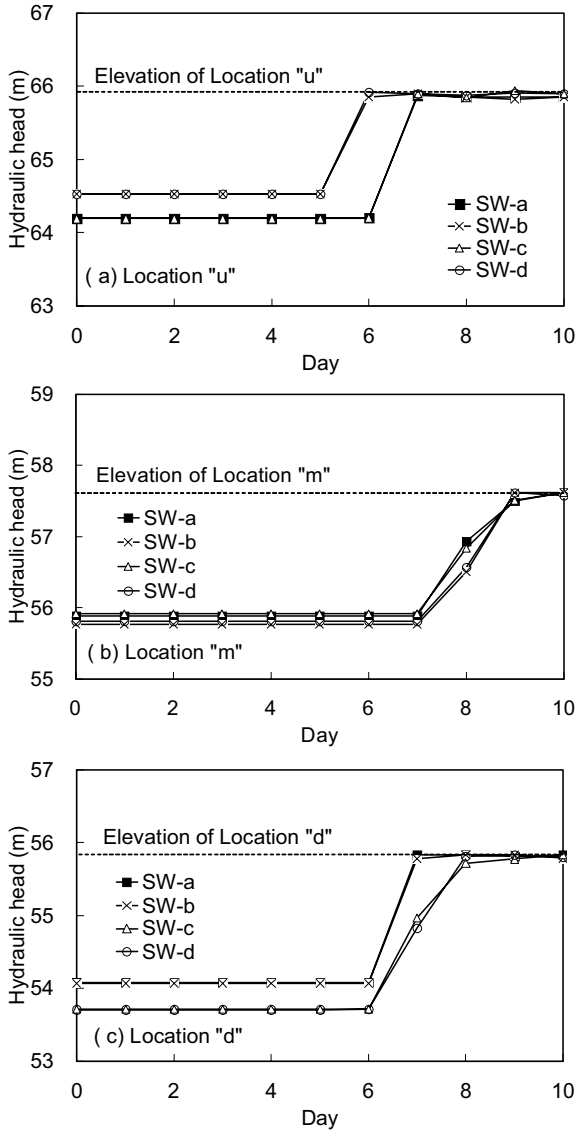

Figure 6. Variations of hydraulic head during the 10-day rainfall

On Day 6, the hydraulic heads of Run SW-b and Run SW-d increase sharply, while the heads of Run SW-a and Run SW-c remain unchanged (see Figure 6a). This is because the wetting fronts in Run SW-b and Run SW-d seeped faster than those in Run SW-a and Run SW-c due to the damming effect, and they reached location “u” first (Figure 7b). Hence, matric suction at location “u” was dissipated (i.e., zero pore water pressure) and hence the hydraulic head at location “u” was equal to the elevation head as shown in Figure 6a. In Run SW-a and Run SW-c, the wetting front has not yet reached location “u” and so the hydraulic heads remain the same as the initial state.

From Day 7 to Day 10, the hydraulic head is almost the same for the four cases considered (see Figure 6a). This is because the wetting front in each analysis has reached and passed through location “u” (Figure 7c) from Day 7 onwards.

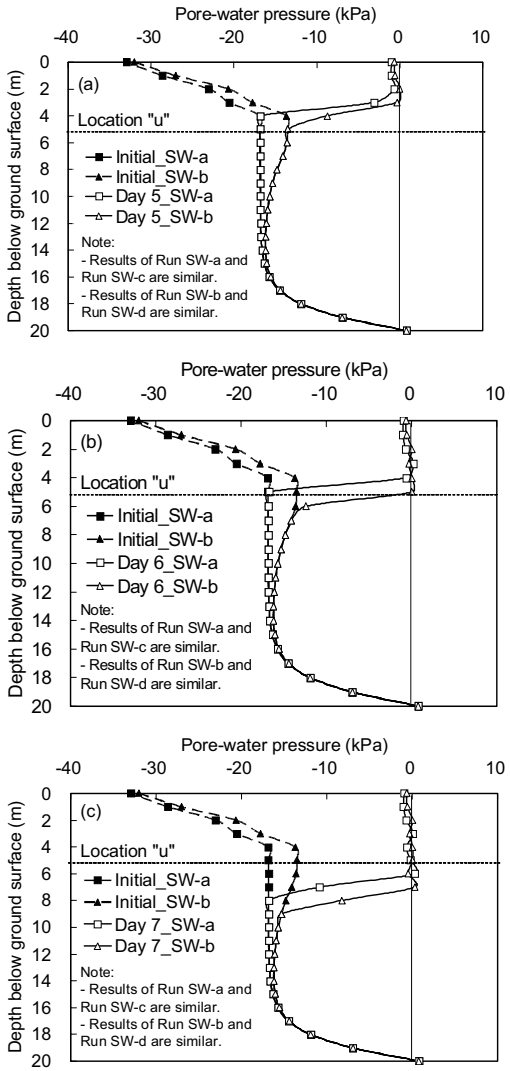

Figure 7. Pore-water pressure distributions at location “u” at (a) Day 5 (b) Day 6 (c) Day 7

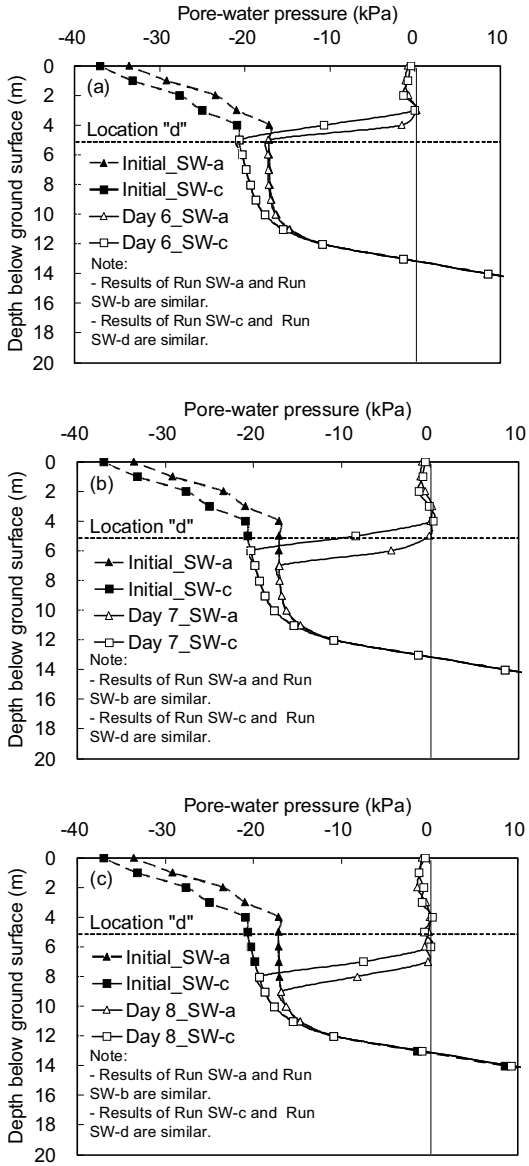

Figure 8. Pore-water pressure distributions at location “d” at (a) Day 6 (b) Day 7 (c) Day 8

Location “m” is situated between Pile One and Pile Two and it is 8m away from both the piles. At this location, there is no significant difference in computed hydraulic head from the four analyses considered during the 10-day rainfall (Figure 6b). This implies that damming does not affect pore-water pressure distribution noticeably at this location.

At location “d”, due to the presence of Pile Two which has dammed seepage from the upstream, the initial hydraulic heads of Run SW-c and Run SW-d are lower than those of Run SW-a and Run SW-b (Figure 6c). From Day 1 to Day 6, no major change in hydraulic head is observed. This is because there is not enough time for wetting fronts to reach location “d” as shown in Figure 8a. The computed wetting fronts from Run SW-c and Run SW-d are shallower than those from Run SW-a and Run SW-b due to damming at the upstream face of Pile Two in the former two runs. On Day 7, hydraulic heads of Run SW-c and Run SW-d increase less than those of Run SW-a and Run SW-b (Figure 6c). This is because the wetting fronts in Run SW-c and Run SW-d have seeped slower than those in Run SW-a and Run SW-b as a result of damming effect (refer to Figure 8b). From Day 8 to Day 10, there is almost no difference in hydraulic head among the four analyses (Figure 6c) because the wetting front in each analysis has reached and passed through location “u” from Day 8 onwards. The hydraulic head at location “u” is equal to the elevation head suggesting that pore water pressure is zero at this location (Figure 8c).

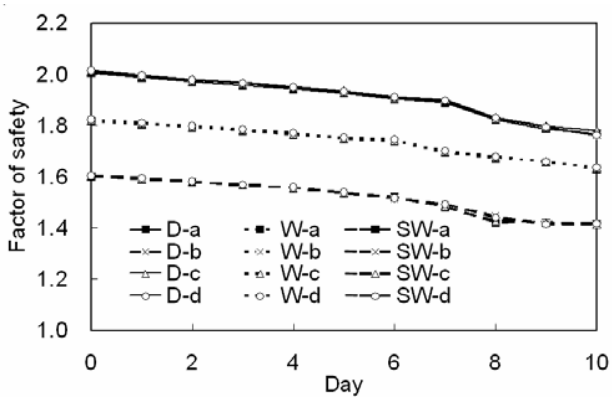

Figure 9. FOSs with respect to time for all analyses

5. VARIATIONS OF SLOPE STABILITY

5.1 Influence of wetting SWCC and SDSWCC

Based on pore water pressures computed by SEEP/W, slope stability analysis of the assumed slip surface (see Figure 4) is carried out using SLOPE/W. Figure 9 shows the variations of FOSs with elapsed time for different cases during the 10-day rainfall. As expected, the computed FOS decreases as time elapses during the 10-day rainfall. It can be seen that the FOSs of the analyses using the drying SWCCs (i.e. Series D) are the highest for a given rainfall condition. On the contrary, the FOSs computed from the analyses using the wetting stress-dependent SDSWCCs (i.e. Series SW) are the lowest. This difference between the two series of analyses is attributed to the significant difference in the computed initial pore-water pressure distributions (Figures 5a to 5c). This implies that an analysis using a drying SWCC would lead to non-conservative or even unsafe predictions.

5.2 Damming effect on slope stability

For the given assumed slip surface, there is no significant difference in the computed FOSs due to damming effects. This is because the pore-water pressure distribution along the assumed slip surface is only slightly affected by damming. Although some damming on pore-water

pressure can be observed at locations “u” and “d”, the effects are not significant (Figures 6a and 6c). At location “m”, the influence of damming is even smaller (Figure 6b). In fact, the extent of damming effects on pore water pressure and slope stability has already been overestimated in this study. This is because the numerical simulations are only two-dimensional. Actual three-dimensional groundwater flow around hydraulic obstacles is not permitted in the two-dimensional analyses. In other words, damming effect on FOSs would be even smaller if a three-dimensional analysis is carried out.

6. CONCLUSIONS

Based on the simplified two-dimensional numerical investigations, the influence of wetting process and stress state on pore-water distributions and factor of safety of an unsaturated soil slope have been investigated. During the 10-day prolonged rainfall, the FOS obtained from a conventional analyses using a drying SWCC is the highest, whereas an analysis using wetting stress-dependent SDSWCCs would predict the most adverse initial pore-water pressure distributions with depth, and hence the lowest FOS. Thus, stress-dependency of SWCC should be considered and used in transient seepage analysis.

For the geometry and ground conditions considered, damming of groundwater due to the presence of pile obstacles is very limited in the two-dimensional space. In other words, damming effects would be even smaller if a three-dimensional analysis is carried out.

7. ACKNOWLEDGMENTS

This research project is supported by research grants HKUST6108/99E and HKUST6087/00E provided by the Research Grants Council of the Hong Kong Government of the Special Administrate Region.

8. REFERENCES

Anderson, M. G. and Pope, R. G. 1984. The incorporation of soil water physics models into geotechnical studies of landslide behavior. Proc., 4th Int. Symp. on Landslides, Vol. 4, pp. 349-353.

Fredlund, D. G. and Barbour, S. L. 1992. Integrated seepage modeling and slope stability analyses: A generalized approach for saturated/unsaturated soils. Geomechanics and water engineering in Environmental Management, edited by Chowdhury, R.H., pp. 3-34

Fredlund, D. G., Morgenstern, N. R., and Widger, R. A. 1978. The shear strength of unsaturated soil. Canadian Geotechnical Journal, Ottawa, Vol. 15, pp. 313– 321.

Fredlund, D. G., Xing, A. and Huang, S. 1994. Predicting the permeability functions for unsaturated soils using the soil-water characteristic curve. Canadian Geotechnical Journal, Ottawa, Vol. 31, pp. 533-546.

Fredlund, D. G. and Xing, A. 1994. Equations for the soil-water characteristic curve. Canadian Geotechnical Journal, Ottawa, Vol. 31, pp. 521–532.

GEOGUIDE 1998. Guide to rock and soil descriptions. Geotechnical Control Office, Public Works Department of Hong Kong, Hong Kong.

Geo-slope, 2002. SEEP/W (Ver. 5) for finite element seepage analysis and SLOPE/W (Ver. 5) for slope stability analysis. Geo-slope International, Canada.

Hilf, J. W. 1956. An investigation of pore-water pressure in compacted cohesive soils, PhD dissertation, Tech. Memo. No. 654, U.S. Dept. of the Interior, Bureau of Reclamation, Design and Construction Division, Denver.

Lam, C. C. and Leung, Y. K. 1995. Extreme rainfall statistics and design rainstorm profiles at selected locations in Hong Kong. Tech. Note No. 86. Royal Observatory, Hong Kong.

Lam, L., Fredlund, D. G. and Barbour, S. L. 1987. Transient seepage model for saturated-unsaturated soil systems: A geotechnical engineering approach. Canadian Geotechnical Journal, Ottawa, Vol. 24, pp. 565–580.

Rahardjo, H. and Leong, E. C. 1997. Soil-Water Characteristic Curves and Flux Boundary Problems. Unsaturated Soil Engineering Practice, edited by Houston, S. L. and Fredlund, D. G., pp. 88-112.

Ng, C. W. W. and Pang, Y. W. 1998. Lai Ping road landslide investigation —Specialist testing of unsaturated soils. Tech. Rep., Geotechnical Engineering Office of the Hong Kong Special Administrative Region, Hong Kong.

Ng, C. W. W. and Pang, Y. W. 2000. Experimental investigations of the soil-water characteristics of a volcanic soil. Canadian Geotechnical Journal, Vol. 37, pp. 1252-1264.

Ng, C. W. W. and Shi, Q. 1998. A numerical investigation of the stability of unsaturated soil slopes subjected to transient seepage. Computers and Geotechnics, Vol. 22, pp. 1-28.

Ng, C.W.W., Wang, B. and Tung, Y.K. 2001. 3D numerical investigations of groundwater responses in an unsaturated slope subjected to various rainfall patterns. Canadian Geotechnical Journal, Ottawa, Vol. 38, No.5, pp. 1049-1062.

SoilVision (Version 3.34). 2002. Soilvision Systems Ltd., Sask., Saskachewan, Canada.

Tung, Y. K., Ng, C. W. W. and Liu, J. K. 1999. Lai Ping road landslide investigation—Three dimensional groundwater flow computation. Technical Report — Part I, Geotechnical Engineering Office of the Hong Kong Special Administrative Region, Hong Kong.